Abnormal Functional and Structural networks in Rectal Cancer with Depressive risk: A Graph Theory Analysis

Wenwen Zhang
Gansu Province People's Hospital
Ying Zou
Lanzhou University
Yuan Li
Shandong Normal University
Yu Fu
Lanzhou University
Jie Shi
Lanzhou University
Gang Huang
Gansu Province People's Hospital
Zhijun Yao
Lanzhou University
Bin Hu (bh@lzu.edu.cn)
Lanzhou University

Research article

Keywords: Rectal cancer, Functional network, Structural network, Multimodal research, Graph theory analysis

Posted Date: December 5th, 2019

DOI: https://doi.org/10.21203/rs.2.12939/v2

Abstract

Background: Surgery and chemotherapy can cause depressive risk in patients with rectal cancer (RC). However, few comprehensive studies are conducted on RC patients associated alterations induced by emotional disorders in the topological organization of structural and functional networks. Methods: Resting-state functional MRI and Diffusion tensor imaging data were collected from 36 RC patients with surgery and chemotherapy and 32 healthy controls (HC). Functional network (FN) was constructed from extracting average time courses for 246 regions of interest (ROI) and structural network (SN) was established by deterministic tractography. Graph theoretical analysis was used to calculate small-worldness property, clustering coefficients, shortest path length and network efficiency. Additionally, we assess network resilient on FN and SN. Results: Abnormal small-worldness property of FN and SN were found in RC patients. The FN and SN exhibited increased local efficiency and global efficiency respectively in RC patients.The increased nodal efficiency in RC patients were mainly found in the frontal lobe, parietal lobe and limbic lobe for FN and SN, while the decreased nodal efficiency were distributed in subcortical nuclei, parietal lobe and limbic lobe only for SN. In network resilient analysis, the RC patients showed less resilient to targeted or random node deletion in both networks compared with HC. Moreover, FN is more robust than SN for all participants. Conclusions: This study revealed that topological organizations of the FN and SN may be disrupted in RC patients. Brain network reorganization is a compensation mechanism to alleviate the depressive risk in RC patients after surgery and chemotherapy.

Background

Rectal cancer (RC) is a disease characterized by a high mortality rate. Patients with RC usually suffer from tremendous psychological stress, which leads to a series of psychological diseases [1, 2]. Some contemporary studies showed that various discomfort symptoms caused by chemotherapy could induce cognitive impairment in cancer patients, including impaired attention, memory and executive function [3, 4]. The long-term emotional distress of the patient increased the risk of depression[5]. Depression-related factors may contribute to the less optimal network topology in the functional network (FN) and structural network (SN) of cancer patients [6, 7]. Neuroimaging studies reported that a considerable number of cancer patients with surgery and chemotherapy had morphological variation and functional abnormalities in brain, such as decreased hippocampal volume [8], lower white matter volume [9], as well as memory difficulties [2] and cognitive deficit [10]. Therefore, research on FN and SN in this study could bring new insights into the neurophysiological mechanisms in RC patients, and through the analysis of brain images, the emotional distress of RC patients could be diagnosed and treated, thereby improving the quality of life of patients[11].

Combining multi-modal data can reveal hidden relationships among different data, unifying different findings in brain imaging [12]. Therefore, multi-modal imaging is a prominent method in cognitive neuroscience research. Graph-based functional and structural brain connectivity analysis is a new method, which provides evidences for the complexity of the brain by modeling the interactions between different brain regions [13]. Previous studies have consistently shown that brain functional networks are organized in a small-worldness property with local specialization and high capacity for global information transfer [14, 15]. Bruno, Hosseini [2] reported significantly reduced shortest path length and small-worldness property in the breast cancer group. Several findings point that the functional network of cancer patients loses its ability to support various cognitive functions following chemotherapy [16, 17]. Observational studies found that alterations in brain structural network had an adverse impact on the cognition of cancer survivors [18, 19]. Although there are many studies on brain cognitive impairment in cancer patients, little is known about FN and SN abnormalities in RC patients. We used multimodal neuroimaging to investigate the alterations in functional and structural connectivity for getting a deep understanding of the brain cognitive dysfunction in cancer patients.

In view of the poor understanding of psychological disorders and cognitive impairment of rectal cancer survivors in existing studies, it is essential to study the depressive risk and related factors in rectal cancer patients. Therefore, the present study investigated abnormalities in FN and SN using graph theory analysis in RC patients with surgery and chemotherapy characterized by depressive risk compared with healthy controls (HC). We hypothesized that RC patients would show altered small-worldness property and topological architecture in the FN and SN due to the effects of depressive risk. We sought to expand our understanding of the resilience of the brain network in RC patients. The study also explored the potential association between the significant alterations in network properties of RC patients and severity of depression symptoms.

Methods

2.1. Participants

36 RC patients were recruited from the Gansu Provincial Hospital, while the 32 age and gender matched healthy control participants were recruited through newspaper advertisements. They were recruited from July 2017 to May 2019. All participants were diagnosed according to DSM-IV criteria by two experienced psychiatrist. They have executed the evaluation of 17-item Hamilton Rating Scale for Depression (HAMD-17). We divided the severity of depression in cancer patients into three categories: HAMD score 1-7 (17 participants), score 8–17 (14 participants), score>17 (5 participants). All participants were given written informed consent when image scanning.

2.2. Data acquisition

MRI data were acquired using a 3.0 T Siemens Trio scanner (Siemens Erlangen, Germany). Subjects were asked to relax with eyes closed and to not think about anything. The structural image was acquired with a T1-weighted spin-echo sequence: TR/TE = 2530/2.98 ms, slice thickness = 1 mm, slice gap = 0.8 mm, FOV=256*256mm, The resting-state functional images (rs-fMRI) were obtained with the following parameters: TR/TE=2000/30ms, 64*64 matrix, FOV=224*224mm, total 240 volumes, 32 sequential ascending axial slices of 3.5 mm thickness. Diffusion tensor imaging (DTI) data were acquired using a singleshot echo-planar imaging-based sequence with the following parameters: TR =11600, TE=85, FOV=256*256mm, acquisition matrix = 112*112, axial slices=32, 64 diffusion directions with b = 1000 s/mm^2, and an additional image without b = 0 s/mm^2.

2.3 Data Processing

All rs-fMRI data were preprocessed using the Statistical Parametric Mapping (SPM8: http://www.fil.ion.ucl.ac.uk/spm) and Data Processing Assistant Resting-State fMRI (DPARSFA; http://www.restfmri.net)[20]. The specific preprocessed steps were as follows: (1) the first 10 volumes of the functional images were removed; (2) slice timing, head motion correction, and realignment were performed; (3) all subjects were excluded if their head motion was great than 2.0 mm maximum displacement in any of the x, y or z directions was great than 2° [21]; (4) the leaved rs-fMRI data of 32 HC and 36 RC patients were spatially normalized to Montreal Neurological Institute (MNI) space by applying the parameters of structural image normalization (resampling voxel size of 3mm×3mm×3mm); (5) smoothing with an 8 mm Gaussian kernel of 8 mm full width at half maximum (FWHM) [22]; (6) nuisance covariates regression including 24 head motion parameters, averaged global, white matter signals and cerebrospinal fluid [23]; (7) removing linear trends;, (8) temporal band-pass filtering (0.01–0.08 Hz) was performed to reduce low-frequency drift and high-frequency physiological noise [24].

The DTI data were preprocessed using PANDA (http://www.nitrc.org/projects/panda) [25] in MATLAB2014a. The specific preprocessed steps were as follows: (1) converting DICOM files into NIfTI images; (2) estimating the brain mask; (3) the images were cropped; (4) correcting for the eddy current effect and head motions; (5) averaging multiple acquisitions; (7) calculating FA metrics.

2.4 Construction of Brain Networks

The nodes of the network were demarcated according to the Human Brainnetome Atlas (246 Atlas) with 210 cortical and 36 subcortical subregions [26]. In each subject, 246 Atlas were used to construct brain networks for further graph theory analysis.

Functional brain network was constructed using GRETNA (www.nitrc.org/projects/gretna/), which is a toolbox for analyzing brain connections. For each subject, a 246*246 temporal correlation matrix was constructed using the mean time series of each region by Pearson's correlation coefficient. In order to convert the data into z-values for normal distribution, Fisher's z-transform was performed to each matrix. A FA weighted symmetric matrix (246*246) was constructed for each participant by deterministic tractography as the structural network for following research. Each matrix represented the white matter network of the cerebral cortex, and each row or column in network represented the brain region of 246 atlas. For each participant, FN and SN were used for further graph analysis.

2.5 Threshold calculation

In order to construct an undirected binary network and make the generated graph metrics stable, it is necessary to be thresholded for the weight of the brain networks. There is no fixed method to determine the threshold in current research. Therefore, in FN, we used sparsity (26% 50%) with a step of 1% [27] to divide the network threshold. Then, we calculated the topological properties of FN in a series of thresholds range. In SN, we use FA (0.2 0.42) with a step of 0.2 as the threshold of the network according to previous study [28]. Because unfully connected networks and highly connected networks have an impact on small-worldness property [29], we use these sparsities to determine the network density reasonably.

2.6 Whole brain network organization

Graph theoretical analyses of the FN and SN in RC patients and HC were calculated with routines from the GRETNA toolbox. The network topological properties at the global levels were calculated, including (1) properties that suggest network segregation of brain, such as the normalized clustering coefficient (γ), the local efficiency ; (2) properties that indicate network integration of the brain, such as the normalized shortest path length(λ), the global efficiency ; (3) small-worldness (δ) property which evaluates the balance of segregation and integration.

The nodal efficiency ( ) measures the ability of a particular node to propagate information with all other nodes in the network. It is considered as the inverse of the harmonic mean of the minimum path length between an index node and all other nodes in the network.

2.8 Network Resilience Analysis

Network resilience refers to the ability to withstand perturbations or failures in the network, which is usually related to the stability of complex networks [30, 31]. In FN and SN, we used random or targeted attacks with fixed sparsity or FA values to evaluate the network resilience, so as to ensure that all anatomical regions were involved in the network, thus minimizing the number of false-positive paths [30]. In targeted attack analysis, the betweenness value of each node in the network were calculated and sorted in descending order. We deleted the nodes in the network in order of betweenness value and calculated the global efficiency of each network after attack [32]. In random attacks analysis, we deleted the nodes of network randomly and calculated the global efficiency of each network after attack.

2.9 Statistical Analysis

The demographic and clinical characteristics of the RC patients and HC were analyzed by Chi square test and two-sample t-tests using SPSS 21. We performed statistical comparisons of topological measures between the two groups using non-parametric permutation tests with 5000 iterations for each sparsity and FA value [33]. For the , the non-parametric permutation tests was repeated at a fixed sparsity (sp=26%) and a FA value (FA=0.42). FDR correction was conducted for all these results. Besides, we used Pearson correlation analyses to explore the correlations in RC patients between nodes with significant difference in and the severity of depression (HAMD score).

Results

3.1 Demographic characteristics

As shown in Table 1, two groups were matched for age (p=0.663), and gender (c2 =1.282, p=0.258). There were significant difference in the HAMD (p<0.001) score between the two groups.

3.2 Global Topology of Functional and Structural networks

For the rs-fMRI datasets, compared with the HC, RC patients showed a higher shortest path length (λ)(Figure1B, sparsity=26%) and unchanged clustering coefficient (γ)（Figure 1A）, which resulted in abnormal small-worldness( ) (Figure 1C). Additionally, RC patients showed increased E_{loc} (Figure 1D, sparsity =26%) and unchanged E_{glob} (Figure 1E).

For the DTI datasets, compared with the HC, RC patients showed increased clustering coefficient (γ)(Figure2A, FA= 0.32), small-worldness( )(Figure2C, FA= 0.32,0.34 and 0.38) and unchanged shortest path length (λ)(Figure1B). Moreover, E_{glob} showed significantly increased in RC patients (Figures 2E, FA=0.28-0.32).

Original P value and the FDR-corrected P value of topological measures for each sparsity in Supplementary materials.

3.3 Regional efficiency analysis

Compared with the HC, RC patients showed that significantly decreased nodal efficiency was only in FN. There were several regions including bilateral basal ganglia, right parahippocampal gyrus, bilateral thalamus, right precuneus, and right lateral occipital cortex. Meanwhile, the increased nodal efficiency was mainly in frontal lobe (orbital gyrus), basal ganglia, left inferior frontal gyrus, left amygdala, bilateral cingulate gyrus, left inferior parietal lobule, and right precentral gyrus in FN and SN for RC patients (p<0.05, after 5000 permutation test, FDR test)(Table 2, Table 3; Figure 3).

3.4 The comparison of network resilience

With the targeted and random attack, a significantly decreased decline of the global efficiency was found in FN and SN (Figure 4). In both networks, the global efficiency of RC patients decreased faster over a wide percentage of removal, which reflected that the networks of RC patients were more fragile. In all subjects, the resilience of structural network is weaker than that of functional network under the same threshold.

3.5 Network properties correlation with depression clinical measurements

We analyzed the correlations between HAMD score and the nodes with significant difference. For FN, mPMtha.R (r=0.389, p=0.023) (Figure 5B), and for SN, LAmyg.L (r=0.440, p=0.01) (Figure 5A).

Discussion

In this study, we explored different topological organizations of FN and SN in RC patients and HC. The findings pointed RC patients displayed altered small-worldness property and global topological organization compared with HC. Moreover, there were regions with significant abnormal being mainly distributed in frontal region, subcortical regions and central region in RC patients. In addition, RC patients showed vulnerable network resilience in both networks, and FN would be more stable than SN across participants.

4.1 Network Properties

Although the global and regional brain network properties in breast cancer and lung cancer patients are reported in neuroimaging research using fMRI [34, 35] and DTI [19], rectal carcinoma is still little. Compared with HC, the functional networks of RC patients displayed a higher shortest path length (λ) and decreased small-worldness( ), reflecting reduced global integration and disrupted organization balance [2, 19]. Our results also revealed increased local efficiency in RC patients. It is a measure of local information transmission among adjacent nodes and therefore an indication of network segregation [36]. Previous studies demonstrated reduced local efficiency, a common measure of the brain network's response to computational attack, associated with breast cancer patients [19, 37]. Due to brain structural damage, decreased local efficiency would affect the fault tolerant ability of brain network. More detail, the result of weakening network fault tolerance is that if a node in the brain is damaged, the connection between previously linked nodes would be greatly affected [38]. Therefore, reduced local efficiency is a risk factor for RC patients. Recently, researchers use graph theory to analyze complex brain functional networks after chemotherapy. It has been proved that chemotherapy-related cognitive deficits were associated with abnormal topological alterations of brain functional and structural network [39-41]. In this study, increased shortest path length and decreased local efficiency in RC patients with surgery and chemotherapy could be seen as a brain compensation mechanism, which included changing the global pathway and adjusting regional activity to preserve a seesaw-like balance of the brain network.

RC patients showed increased clustering coefficients (γ), small-worldness( ) and global efficiency in SN (Figure 2). Abnormal small-worldness property of SN indicated that the local specialization and global integration of brain in RC patients were disrupted, where the SN tended to be more randomized[42]. Global efficiency is the inverse of the average shortest path between nodes. When nodes could interact directly, the efficiency is high [19]. Therefore, global efficiency is an indicator of network function integration and parallel information processing capability [38]. The present results of abnormal network properties reflected the undesired topological organization in SN, which exhibited that the deficits of emotional and cognitive processing in RC patients might result from network damages. Besides, the increased network properties of SN in RC patients might suggest that local nerve fibers reconstructed in response to the abnormalities in brain functional network. The compensatory response of the SN is activated for maintaining brain functional integrity to compensate the cognitive

impairment caused by chemotherapy to RC patients [43]. Aforementioned evidences illuminated that cognitive deficit related to RC patients may act via disrupted coordination between global and regional networks.

4.2 Regional nodal parameters

To explore the functional and structural characteristics of the human brain more accurately and quantitatively, our study employed a new standard brain atlas, containing 246 brain regions. This atlas would allow brain network analysis to use predefined nodes in an informed manner [44]. Therefore, more detailed division of brain regions provide better help in multi-modal data analysis. We observed decreased only in FN of RC patients. The significantly changed regions were located in bilateral basal ganglia, bilateral thalamus, right parahippocampal gyrus, right precuneus, and right lateral occipital cortex. The basal ganglia is not only related to motor control, but also related to the cognitive and limbic functions [44]. Moreover, basal ganglia is the collection of subcortical nuclei surrounding the thalamus [45]. Abnormal activation of basal ganglia/thalamus was found in the depressive studies [46, 47], suggesting that abnormalities in these brain regions may lead to abnormal emotional processing mechanisms. Prior studies reported that parahippocampal gyrus and precuneus were associated with memory function, so alterations in these regions might affect memory decline [48, 49]. Task-fmri study of memory factors found that the occipital cortex of cancer patients was more significantly correlated with vigor and fatigue scores [50]. Frequent fatigue is a common symptom of cancer patients [51]. Aforementioned evidences indicated that the decreased of FN in this study represented alterations in regional characteristics of the brain network, which further affected the cognitive impairment of RC patients.

Furthermore, the increased nodal efficiency was mainly in frontal cortex, left amygdala, bilateral cingulate gyrus, left inferior parietal lobule, and right precentral gyrus in FN and SN for RC cancer patients. In experiments with high-demand condition, the right inferior frontal gyrus as well as other components of the two hemisphere working memory circuitry in cancer patients were found greater activation than the control group in a prior study [52]. These abnormalities might be a compensation mechanism to preserve normal thinking and responsiveness in cancer patients. In addition, chemotherapy affects estrogen levels in cancer patients. Estrogen levels are thought to have neuroprotective effects in the brain, thus helping to maintain cognitive function [53]. Therefore, female cancer patients are more likely to develop cognitive impairment in brain regions related to learning and memory after chemotherapy, such as hippocampus and amygdala [54]. The anterior cingulate cortex is involved in attention control, response selection and error monitoring [55]. Abnormal brain activity patterns in the attention-controlled regions, including the anterior cingulate gyrus, are related with anxiety [56]. The emotional fluctuation caused by excessive psychological stress in RC patients could induce abnormal activation of cingulate gyrus. Saykin, McDonald [57] revealed that the activation of frontal and parietal lobes increased during the speech working memory task 1 month after chemotherapy. Compared with controls, the cancer group showed significantly greater activation in right precentral gyrus, right cingulate gyrus [17]. Moreover, in the SN, the nodal efficiency were only increased. We speculated that after surgery and chemotherapy, the node efficiency of SN showed more obvious activation in order to maintain robustness of overall network at the expense of other network property, such as integration. These results improved the understanding of chemotherapy-induced cognitive impairment in RC patients from the perspective of brain node efficiency.

As shown in Figure 5, the RC patients showed a positive relationship between HAMD and decreased nodal efficiency in mPMtha.R of FN, as well as a positive relationship between HAMD and increased nodal efficiency in LAmyg.L of SN. The correlation between the changed node efficiency and HAMD score may indicate impaired cognitive control combined with abnormal affective processing in RC patients[58]. A prior study suggested that regions sensitive to negative emotions were hyperactive in processing negative information[59], it was not surprising to find a significant positive correlation between increased nodal efficiency and HAMD in the amygdala. Moreover, the positive relationship between HAMD and decreased nodal efficiency revealed that abnormal activation of FN in RC patients might cause cognitive impairments and depressed mood[60]. Therefore, we speculated that alterations in brain network properties assist us to study the depressive risk in RC patients after chemotherapy and surgery.

4.3 The difference of network resilience

In both networks, a key finding of significantly decreased resilience to targeted and random attack was found (Figure 4). Being more effective than other network properties to measure network integration performance, global efficiency of the FN and SN were utilized to explore network resilience quantitatively [32]. In the present study, both networks of RC patients were more vulnerable and SN is less resilient than FN, which were consistent with our previous research results [61]. This finding enhanced the conclusion that lower brain resilience was associated with progressive deterioration of cognitive impairment in breast cancer survivors [19]. Similar results were investigated in other neurological diseases such as major depressive disorders [31] and temporal lobe epilepsy [30]. A previous study showed that the degree distribution of brain network followed the exponentially truncated power law [62]. This exponentially truncated power law distribution may be helpful in resisting the targeted attack of the hubs, meaning the brain networks of two groups were almost constant when deletion rate was low [63]. The deletion ratios reaching 50%, the decline rate of global efficiency in networks began to exhibit obvious differences. Exploring the resilient of networks actually simulated the process of cognitive decline in all participants. In detail, as the important nodes were deleted, the functional and structural integrity of brain networks were impaired. Additionally, the FN was more resilient than the SN in present study, which were similar with these findings in previous studies [28, 64]. A prior study discovered that there was commonly a functional connectivity between regions that have no direct structural connectivity, implying that functional network was a more stable system in brain network [65]. Therefore, functional networks were more robust to node removal. Our results may provide a new direction for studying cognitive impairment in RC patients after surgery and chemotherapy.

Conclusions

The present study uncovers the effects of depression symptoms on brain functional and structural network in RC patients with surgery and chemotherapy through multimodal brain connectivity analysis. RC patients show the abnormal small-worldness property and network topological organization in FN and SN. The alterations in nodal parameter are mainly observed in the limbic and parietal lobes as well as the subcortical nuclei in RC patients. The RC patients demonstrate significant cognitive impairment compared with HC and this impairment may be associated with lower network attack tolerance. The discovery

of functional and structural networks is critical for understanding the neurobiological mechanism associated with depressive symptoms in RC patients with surgery and chemotherapy.

Limitations

The cross-sectional study limited the ability of studying the causal relationship between alterations in brain network and depressive symptoms of RC patients. The statistical power is restricted by small sample size to some extent. Finally, this study lacks the joint analysis for multimodal data. It is very meaningful to use different modal data for fusion research.

Abbreviations

vmPu: ventromedial putamen; dCa: dorsal caudate; GP: globus pallidus; TL: area TL (lateral PPHC, posterior parahippocampal gyrus); PPtha: posterior parietal thalamus; lPFtha: lateral pre-frontal thalamus; vCa: ventral caudate; A7m: medial area 7(PEp); Otha: occipital thalamus; mPMtha: pre-motor thalamus; msOccG: medial superior occipital gyrus; mPFtha: medial pre-frontal thalamus; L: left; R: right. A12/47l : lateral area 12/47; dlPu: dorsolateral putamen; A44op：opercular area 44；A32sg: subgenual area 32; LAmyg : lateral amygdala; L: left; R: right.

Declarations

Acknowledgments

We thank the staff of the Department of Radiology of the Gansu Provincial Hospital for their assistance in collecting the data. We thank all participants for their contributions to this article.

Funding

This work was supported in part by the National Natural Science Foundation of China (Grant No.61632014, No.61627808, No.61210010), in part by the National Basic Research Program of China (973 Program) under Grant 2014CB744600, and in part by the Program of Beijing Municipal Science & Technology Commission under Grant Z171100000117005. Gansu Provincial Hospital Youth Research Fund Project, 18GSSY5-5.

Author Contributions

Conceived and designed the experiments: WZ, YZ, GH, ZY, BH. Analyzed the data: WZ, YZ. Contributed reagents/materials/analysis tools:WZ, YZ, YL, YF, JS, GH, ZY, BH. Wrote the paper: WZ,YZ. All authors contributed to and have approved the final manuscript.

Ethics approval and consent to participate

All participants provided written informed consent at the time of enrollment for image scanning. The research protocol has been approved by the Gansu Provincial Hospital Ethics Committee.

Consent for publication

Not applicable.

Competing Interests

All authors declared no conflict of interest.

Availability of data and materials

The datasets used and/or analysed dudring the current study are available from the correspoding author on reasonable request.

References

1. Li, M. and J. Gu, *Changing patterns of colorectal cancer in China over a period of 20 years.* World journal of gastroenterology: WJG, 2005. **11**(30): p. 4685.
2. Bruno, J., S.H. Hosseini, and S. Kesler, *Altered resting state functional brain network topology in chemotherapy-treated breast cancer survivors.* Neurobiology of disease, 2012. **48**(3): p. 329-338.
3. Wefel, J.S., et al., *Clinical characteristics, pathophysiology, and management of noncentral nervous system cancer-related cognitive impairment in adults.* CA: a cancer journal for clinicians, 2015. **65**(2): p. 123-138.
4. Morean, D.F., L. O'Dwyer, and L.R. Cherney, *Therapies for cognitive deficits associated with chemotherapy for breast cancer: a systematic review of objective outcomes.* Archives of physical medicine and rehabilitation, 2015. **96**(10): p. 1880-1897.
5. Linden, W., et al., *Anxiety and depression after cancer diagnosis: prevalence rates by cancer type, gender, and age.* Journal of affective disorders, 2012. **141**(2-3): p. 343-351.
6. Kesler, S.R., et al., *Predicting long-term cognitive outcome following breast cancer with pre-treatment resting state fMRI and random forest machine learning.* Frontiers in human neuroscience, 2017. **11**: p. 555.

7. Billiet, T., et al., *Recovery from chemotherapy-induced white matter changes in young breast cancer survivors?* Brain imaging and behavior, 2018. **12**(1): p. 64-77.
8. Eberling, J.L., et al., *Estrogen-and tamoxifen-associated effects on brain structure and function.* Neuroimage, 2004. **21**(1): p. 364-371.
9. McDonald, B.C. and A.J. Saykin, *Alterations in brain structure related to breast cancer and its treatment: chemotherapy and other considerations.* Brain imaging and behavior, 2013. **7**(4): p. 374-387.
10. Janelsins, M.C., et al. *An update on cancer-and chemotherapy-related cognitive dysfunction: current status.* in *Seminars in oncology*. 2011. Elsevier.
11. Vahdaninia, M., S. Omidvari, and A. Montazeri, *What do predict anxiety and depression in breast cancer patients? A follow-up study.* Social psychiatry and psychiatric epidemiology, 2010. **45**(3): p. 355-361.
12. Plis, S.M., et al., *Effective connectivity analysis of fMRI and MEG data collected under identical paradigms.* Computers in biology and medicine, 2011. **41**(12): p. 1156-1165.
13. Spisák, T., et al. *BrainCON: graph theory based multimodal brain connectivity analysis and visualization software.* 2013. European Congress of Radiology 2013.
14. Bullmore, E.T. and D.S. Bassett, *Brain graphs: graphical models of the human brain connectome.* Annual review of clinical psychology, 2011. **7**: p. 113-140.
15. Sporns, O., *The human connectome: a complex network.* Annals of the New York Academy of Sciences, 2011. **1224**(1): p. 109-125.
16. Cimprich, B., et al., *Prechemotherapy alterations in brain function in women with breast cancer.* Journal of clinical and experimental neuropsychology, 2010. **32**(3): p. 324-331.
17. Kesler, S.R., et al., *Regional brain activation during verbal declarative memory in metastatic breast cancer.* Clinical Cancer Research, 2009. **15**(21): p. 6665-6673.
18. Amidi, A., et al., *Changes in brain structural networks and cognitive functions in testicular cancer patients receiving cisplatin-based chemotherapy.* JNCI: Journal of the National Cancer Institute, 2017. **109**(12): p. djx085.
19. Kesler, S.R., C.L. Watson, and D.W. Blayney, *Brain network alterations and vulnerability to simulated neurodegeneration in breast cancer.* Neurobiology of aging, 2015. **36**(8): p. 2429-2442.
20. Yan, C. and Y. Zang, *DPARSF: a MATLAB toolbox for" pipeline" data analysis of resting-state fMRI.* Frontiers in systems neuroscience, 2010. **4**: p. 13.
21. Wang, J., et al., *Graph theoretical analysis reveals disrupted topological properties of whole brain functional networks in temporal lobe epilepsy.* Clinical Neurophysiology, 2014. **125**(9): p. 1744-1756.
22. Liu, F., et al., *Abnormal amplitude low-frequency oscillations in medication-naive, first-episode patients with major depressive disorder: a resting-state fMRI study.* Journal of affective disorders, 2013. **146**(3): p. 401-406.
23. Zeng, L.L., et al., *Unsupervised classification of major depression using functional connectivity MRI.* Human brain mapping, 2014. **35**(4): p. 1630-1641.
24. Wang, L., et al., *Overlapping and segregated resting-state functional connectivity in patients with major depressive disorder with and without childhood neglect.* Human brain mapping, 2014. **35**(4): p. 1154-1166.
25. Cui, Z., et al., *PANDA: a pipeline toolbox for analyzing brain diffusion images.* Frontiers in human neuroscience, 2013. **7**: p. 42.
26. Fan, L., et al., *The human brainnetome atlas: a new brain atlas based on connectional architecture.* Cerebral cortex, 2016. **26**(8): p. 3508-3526.
27. Guo, H., et al., *Resting-state functional connectivity abnormalities in first-onset unmedicated depression.* Neural regeneration research, 2014. **9**(2): p. 153.
28. Jiang, W., et al., *Disrupted structural and Functional networks and Their correlation with alertness in right Temporal lobe epilepsy: a graph Theory study.* Frontiers in neurology, 2017. **8**: p. 179.
29. Braun, U., et al., *Test–retest reliability of resting-state connectivity network characteristics using fMRI and graph theoretical measures.* Neuroimage, 2012. **59**(2): p. 1404-1412.
30. Bernhardt, B.C., et al., *Graph-theoretical analysis reveals disrupted small-world organization of cortical thickness correlation networks in temporal lobe epilepsy.* Cerebral cortex, 2011. **21**(9): p. 2147-2157.
31. Ajilore, O., et al., *Graph theory analysis of cortical-subcortical networks in late-life depression.* The American Journal of Geriatric Psychiatry, 2014. **22**(2): p. 195-206.
32. Rubinov, M. and O. Sporns, *Complex network measures of brain connectivity: uses and interpretations.* Neuroimage, 2010. **52**(3): p. 1059-1069.
33. Yao, Z., et al., *Abnormal cortical networks in mild cognitive impairment and Alzheimer's disease.* PLoS computational biology, 2010. **6**(11): p. e1001006.
34. Murray, E.A., S.P. Wise, and W.C. Drevets, *Localization of dysfunction in major depressive disorder: prefrontal cortex and amygdala.* Biological psychiatry, 2011. **69**(12): p. e43-e54.
35. Bromis, K., et al., *Altered brain functional connectivity in small-cell lung Cancer patients after chemotherapy treatment: A resting-state fMRI study.* Computational and mathematical methods in medicine, 2017. **2017**.
36. Yu, M., et al., *Statistical harmonization corrects site effects in functional connectivity measurements from multi-site fMRI data.* Human brain mapping, 2018. **39**(11): p. 4213-4227.
37. Santarnecchi, E., S. Rossi, and A. Rossi, *The smarter, the stronger: intelligence level correlates with brain resilience to systematic insults.* Cortex, 2015. **64**: p. 293-309.
38. Latora, V. and M. Marchiori, *Efficient behavior of small-world networks.* Physical review letters, 2001. **87**(19): p. 198701.
39. Kesler, S.R., et al., *Disrupted brain network functional dynamics and hyper-correlation of structural and functional connectome topology in patients with breast cancer prior to treatment.* Brain and behavior, 2017. **7**(3): p. e00643.

40. Piccirillo, J.F., et al., *Cognitive impairment after chemotherapy related to atypical network architecture for executive control.* Oncology, 2015. **88**(6): p. 360-368.
41. Deprez, S., et al., *Diffusion tensor MRI of chemotherapy-induced cognitive impairment in non-CNS cancer patients: a review.* Brain imaging and behavior, 2013. **7**(4): p. 409-435.
42. Zhang, J., et al., *Disrupted brain connectivity networks in drug-naive, first-episode major depressive disorder.* Biological psychiatry, 2011. **70**(4): p. 334-342.
43. Feng, Y., et al., *Chemotherapy-induced brain changes in breast cancer survivors: evaluation with multimodality magnetic resonance imaging.* Brain imaging and behavior, 2019: p. 1-16.
44. de Reus, M.A. and M.P. Van den Heuvel, *The parcellation-based connectome: limitations and extensions.* Neuroimage, 2013. **80**: p. 397-404.
45. Jaworska, N., et al., *A review of fMRI studies during visual emotive processing in major depressive disorder.* The World Journal of Biological Psychiatry, 2015. **16**(7): p. 448-471.
46. Kumari, V., et al., *Neural abnormalities during cognitive generation of affect in treatment-resistant depression.* Biological psychiatry, 2003. **54**(8): p. 777-791.
47. Haroon, E., et al., *Conceptual convergence: increased inflammation is associated with increased basal ganglia glutamate in patients with major depression.* Molecular psychiatry, 2016. **21**(10): p. 1351.
48. Ploner, C.J., et al., *Lesions affecting the parahippocampal cortex yield spatial memory deficits in humans.* Cerebral Cortex, 2000. **10**(12): p. 1211-1216.
49. Shipman, S.L. and R.S. Astur, *Factors affecting the hippocampal BOLD response during spatial memory.* Behavioural brain research, 2008. **187**(2): p. 433-441.
50. Zunini, R.A.L., et al., *Differences in verbal memory retrieval in breast cancer chemotherapy patients compared to healthy controls: a prospective fMRI study.* Brain Imaging and Behavior, 2013. **7**(4): p. 460-477.
51. Servaes, P., C. Verhagen, and G. Bleijenberg, *Fatigue in cancer patients during and after treatment: prevalence, correlates and interventions.* European journal of cancer, 2002. **38**(1): p. 27-43.
52. Scherling, C.S., et al., *Pre-chemotherapy differences in visuospatial working memory in breast cancer patients compared to controls: an FMRI study.* Frontiers in human neuroscience, 2011. **5**: p. 122.
53. Goodwin, P.J., et al., *Risk of menopause during the first year after breast cancer diagnosis.* Journal of Clinical Oncology, 1999. **17**(8): p. 2365-2365.
54. McEwen, B., *Estrogen actions throughout the brain.* Recent progress in hormone research, 2002. **57**: p. 357-384.
55. Devinsky, O., M.J. Morrell, and B.A. Vogt, *Contributions of anterior cingulate cortex to behaviour.* Brain, 1995. **118**(1): p. 279-306.
56. EngElS, A.S., et al., *Co-occurring anxiety influences patterns of brain activity in depression.* Cognitive, Affective, & Behavioral Neuroscience, 2010. **10**(1): p. 141-156.
57. Saykin, A., et al. *Altered brain activation following systemic chemotherapy for breast cancer: interim analysis from a prospective fMRI study*. in *Abstract presented at 34th Annual Meeting of the International Neuropsychological Society*. 2006.
58. Guo, W.-b., et al., *Altered white matter integrity of forebrain in treatment-resistant depression: A diffusion tensor imaging study with tract-based spatial statistics.* Progress in Neuro-Psychopharmacology & Biological Psychiatry. **38**(2).
59. Murray, E.A., S.P. Wise, and W.C. Drevets, *Localization of Dysfunction in Major Depressive Disorder: Prefrontal Cortex and Amygdala.* Biological Psychiatry. **69**(12): p. e43-e54.
60. Bürger, C., et al., *Differential abnormal pattern of anterior cingulate gyrus activation in unipolar and bipolar depression: an fMRI and pattern classification approach.* Neuropsychopharmacology, 2017. **42**(7): p. 1399.
61. Yao, Z., et al., *Structural alterations of the brain preceded functional alterations in major depressive disorder patients: Evidence from multimodal connectivity.* Journal of affective disorders, 2019. **253**: p. 107-117.
62. Joyce, K.E., S. Hayasaka, and P.J. Laurienti, *The human functional brain network demonstrates structural and dynamical resilience to targeted attack.* PLoS computational biology, 2013. **9**(1): p. e1002885.
63. Friedman, E.J. and A.S. Landsberg, *Hierarchical networks, power laws, and neuronal avalanches.* Chaos: An Interdisciplinary Journal of Nonlinear Science, 2013. **23**(1): p. 013135.
64. Damoiseaux, J.S., et al., *Consistent resting-state networks across healthy subjects.* Proceedings of the national academy of sciences, 2006. **103**(37): p. 13848-13853.
65. Honey, C., et al., *Predicting human resting-state functional connectivity from structural connectivity.* Proceedings of the National Academy of Sciences, 2009. **106**(6): p. 2035-2040.

Tables

Table 1 Demographic and clinical characteristics of subjects.

Variables(Mean±SD)	RC patients (n=36)	Healthy controls (n=32)	p-value
Gender(M:F)	21:15	19:13	0.564#
Age(years)	50.89 ± 7.50	48.96 ± 7.93	0.756*
HAMD	8.94 ± 4.93	_	_

Abbreviations: SD=standard deviation, HAMD= Hamilton depression rating scale. # and * indicate p value for chi-square test and two-sample t-test, respectively.

Table 2 Brain regions with significant group effect in the nodal efficiency between RC patients and HC for FN.

	Regions	Post	Control	P-value
RC<HC				
	vmPu.R	0.5580±0.0582	0.6190±0.0578	0.0002
	dCa.L	0.5116±0.0694	0.5816±0.0592	0.0002
	GP.R	0.5575±0.0732	0.6195±0.0526	0.0002
	vmPu.L	0.5765±0.0490	0.6264±0.0542	0.0002
	TL.R	0.5874±0.0466	0.5941±0.0533	0.0008
	PPtha.R	0.5245±0.0737	0.5846±0.0519	0.0004
	GP.L	0.5581±0.0661	0.6107±0.0620	0.0006
	lPFtha.R	0.5645±0.0698	0.6148±0.0589	0.0032
	vCa.R	0.5223±0.0507	0.5645±0.0514	0.0044
	A7m.R	0.6101±0.0540	0.6404±0.0656	0.0060
	Otha.R	0.5318±0.0491	0.5833±0.0610	0.0052
	mPMtha.R	0.5719±0.0416	0.6158±0.0542	0.0060
	msOccG.R	0.6029±0.0705	0.6429±0.0569	0.0098
	dCa.R	0.5286±0.0650	0.5701±0.0647	0.0090
	mPFtha.R	0.5545±0.0615	0.6007±0.0778	0.0090
RC>HC				
	A23v.L	0.6719±0.0485	0.6601±0.0612	0.0018
	A40rd.L	0.6862±0.0527	0.6738±0.0686	0.0042
	A40rv.L	0.7195±0.0408	0.6875±0.0388	0.0048
	A23v,R	0.6742±0.0394	0.6360±0.0479	0.0064
	A4tl.R	0.7038±0.0857	0.6709±0.0631	0.0048

Table 3 Brain regions with significant group effect in the nodal efficiency between RC patients and HC for SN.

	Regions	Post	Control	P-value
RC>HC				
	A12/47l.L	0.2498±0.0352	0.2099±0.0717	0.0036
	dlPu.L	0.3117±0.0386	0.2774±0.0610	0.0036
	A44op.L	0.2461±0.0316	0.2105±0.0698	0.0054
	A32sg.L	0.2365±0.0365	0.1857±0.0993	0.0062
	LAmyg.L	0.2589±0.0269	0.2148±0.0923	0.0086

Figures

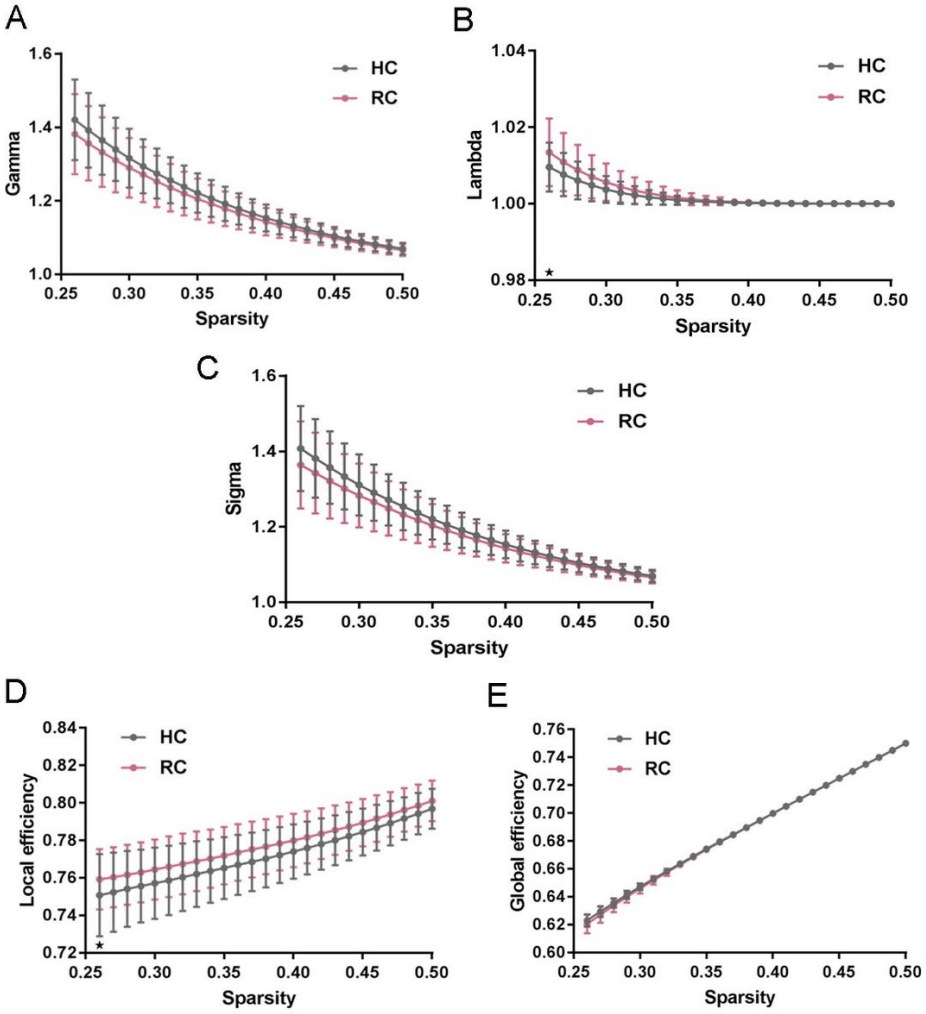

Figure 1

Functional connectivity network at different sparsity for RC patients (the pink line) and controls (the gray line) and their statistical comparison results ($p<0.05$ 5000 permutation test, FDR correction). (A) Gamma, (B) lambda, (C) sigma, (D) local efficiency, (E) global efficiency. The black stars indicate a significant group difference.

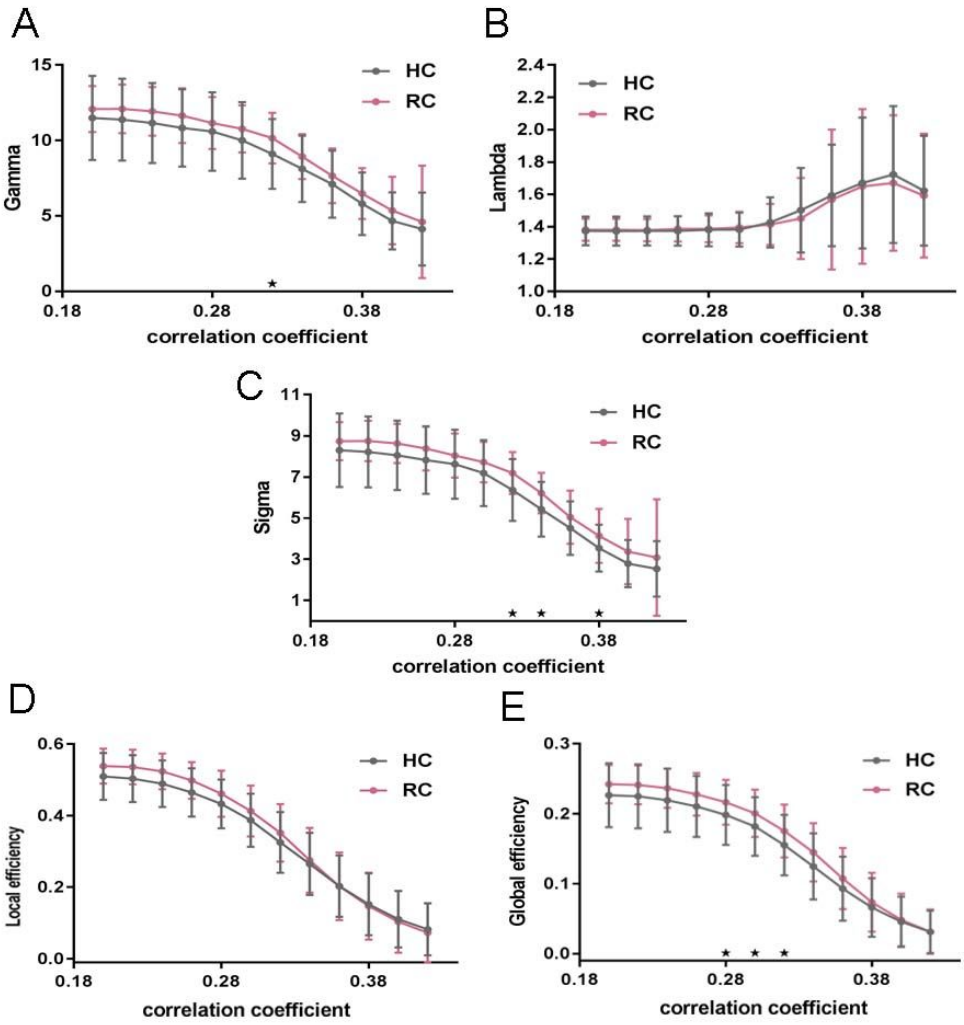

Figure 2

Structural connectivity network at different FA threshold for RC (the pink line) and controls (the gray line) and their statistical comparison results ($p<0.05$ 5000 permutation test, FDR correction). (A) Gamma, (B) lambda, (C) sigma, (D) local efficiency, (E) global efficiency. The black stars indicate a significant group difference.

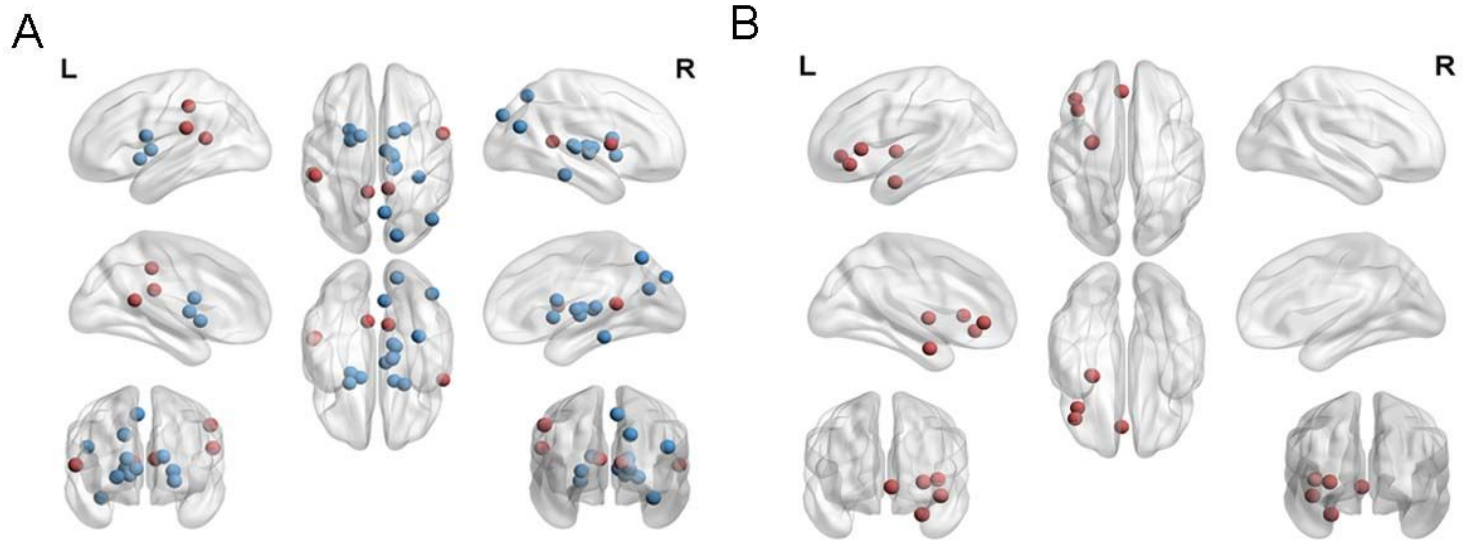

Figure 3

Regions with significant differences in nodal efficiency between RC patients and HC. Nonparametric permutation tests were applied to nodal efficiency of all 246 cortical regions ($p < 0.05$ 5000 permutation test, FDR correction). A represented FN, and B represented SN. Red is for increased nodal efficiency in RC patients group, while blue is for decreased nodal efficiency in RC patients group. L=left; R=right.

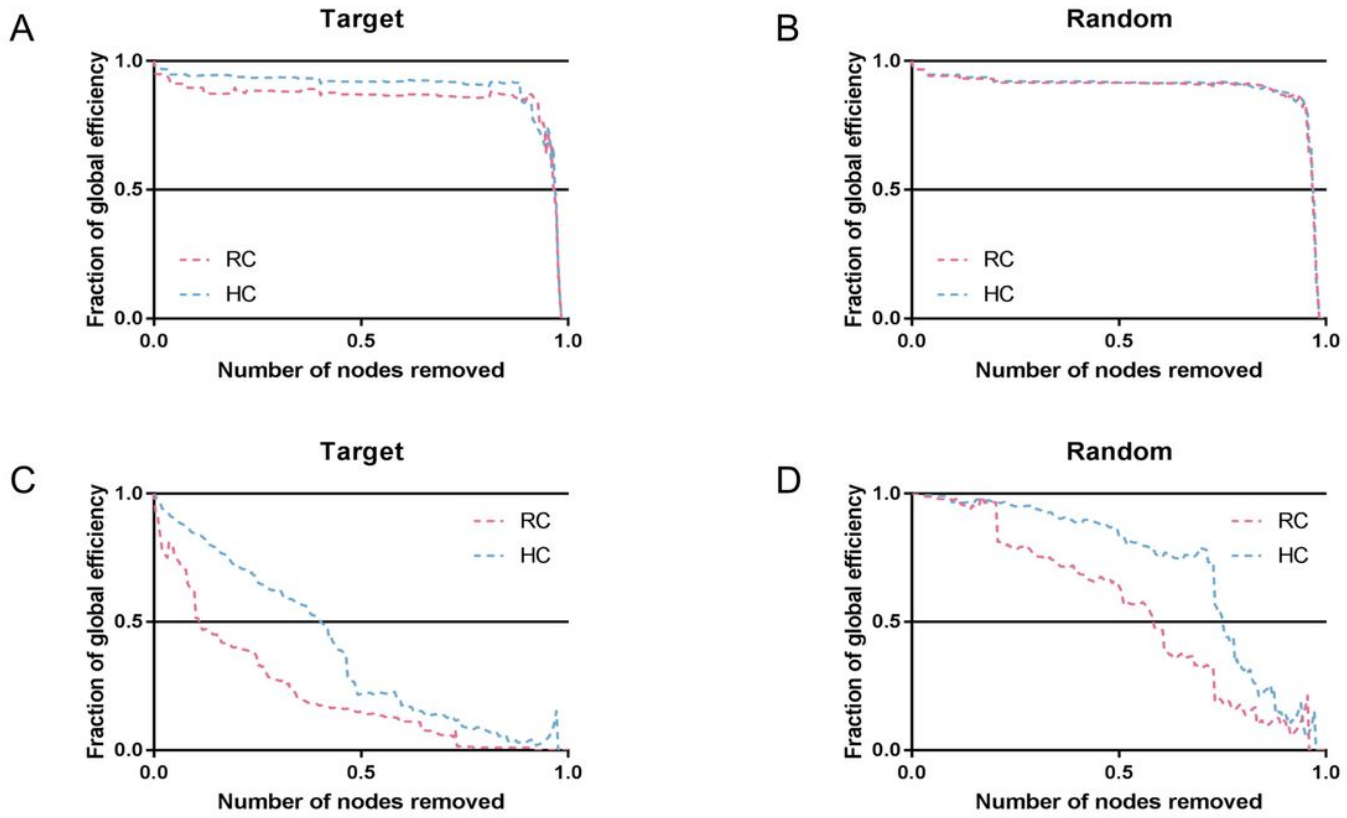

Figure 4

Network resilience under random and target analysis. The alterations of global efficiency under removing node at random (right panel) and targeted pattern (left panel). The pink line corresponded to the performance of HC, blue line for MDD.

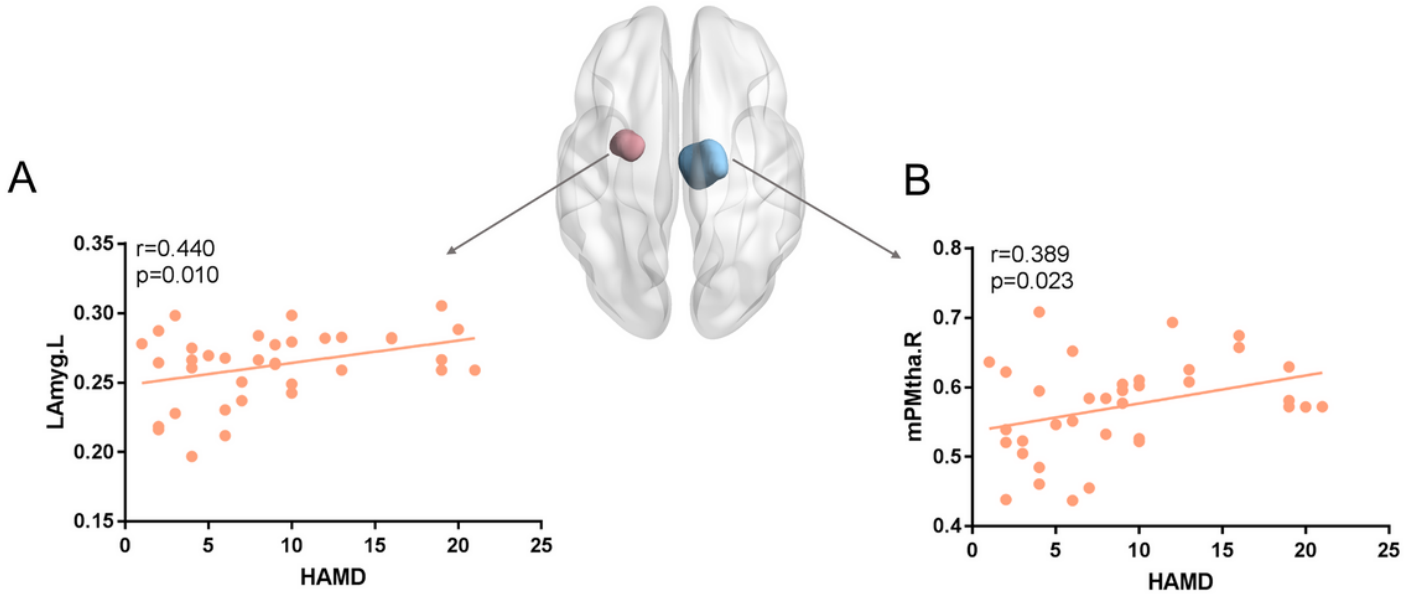

Figure 5

The nodal efficiency of several regions were positively correlated with the HAMD score for FN and SN. The brain map showed regions with decreased Enod (Blue for mPMtha R and pink for LAmygL) Abbreviations: MPFtha: medial pre-frontal thalamus; LAmyg: lateral amygdala; L: left; R: right.